

## Scaling of electronic probability densities in a single-electron tunnelling phenomenon

This article has been downloaded from IOPscience. Please scroll down to see the full text article.

2000 J. Phys. A: Math. Gen. 33 7873

(<http://iopscience.iop.org/0305-4470/33/44/303>)

View [the table of contents for this issue](#), or go to the [journal homepage](#) for more

Download details:

IP Address: 171.66.16.123

The article was downloaded on 02/06/2010 at 08:35

Please note that [terms and conditions apply](#).

## Scaling of electronic probability densities in a single-electron tunnelling phenomenon

Y Kodama<sup>†</sup> and T Maekawa<sup>‡§</sup>

<sup>†</sup> Research Centre of Computational Mechanics, Inc

<sup>‡</sup> Bio-Nano Electronics Research Centre, Toyo University, 2100 Kujirai, Kawagoe, Saitama 350-8585, Japan

Received 25 April 2000, in final form 25 August 2000

**Abstract.** We studied electronic tunnelling through a potential barrier between two quantum wells in one- and two-electron systems numerically. We solved a one-dimensional Schrödinger eigenvalue equation by the QL and finite difference methods. We found that taking  $E - E_c$  as the control parameter, where  $E$  is the strength of the external electric field and  $E_c$  is the tunnelling electric field, power laws apply to the tunnelling probability, the first moment and the second moment for both one- and two-electron systems. We carried out a scaling analysis of the electronic tunnelling problem and found that the amount of increase or decrease in the probability density of electron in each quantum well is scaled. We derived the relationship between the scaling exponents, which agreed with the numerical result. We also found that in the case of two-electron systems, the system energy and the information entropy change discontinuously when an electron tunnels, whereas in the case of one-electron systems, they change continuously in the tunnelling electric field.

### 1. Introduction

Recent remarkable progress in ultra-fine processing technologies has enabled us to process mesoscopic structures and design quantum devices [1, 2]. In a mesoscopic region, electrons show their wave characteristics and the transport mode becomes almost ballistic. Several mesoscopic devices, in which quantum characteristics are utilized, are proposed [3–5]. A single-electron tunnelling (SET) device is one of them, the electronic performances of which have been intensively investigated experimentally in recent years [6–10].

Since an electron is able to tunnel through a potential barrier in a particular strength of electric field, there may be a similarity between electronic tunnelling phenomenon and a critical phenomenon such as percolation [11], although there is a crucial difference between them, that is, resonant electronic tunnelling occurs between finite-sized quantum wells (quantum wells) or dots, whereas critical phenomena occur in an infinite thermodynamic system. First, let us summarise the classical percolation scaling for a later analysis of the electronic tunnelling problem. In the case of a classical percolation system, the number of clusters which are composed of  $s$  particles,  $n_s$ , is scaled as follows:

$$n_s(p) \sim s^{-\tau} f[(p - p_c)s^\sigma] \quad (1)$$

where  $s$  and  $p$  are, respectively, the number of particles in a cluster and the percolation probability.  $p_c$  is the critical percolation probability, and  $\tau$  and  $\sigma$  are the critical exponents.

§ Corresponding author.

In this case, power laws apply to the zeroth moment  $M_0$ , first moment  $M_1$  and second moment  $M_2$ , as follows:

$$M_0 \equiv \sum_s n_s \sim |p - p_c|^{\frac{\tau-1}{\sigma}} \quad (2)$$

$$M_1 \equiv \sum_s s n_s \sim |p - p_c|^{\frac{\tau-2}{\sigma}} \quad (3)$$

$$M_2 \equiv \sum_s s^2 n_s \sim |p - p_c|^{\frac{\tau-3}{\sigma}} \quad (4)$$

where  $M_0$ ,  $M_1$  and  $M_2$  correspond to the total number of clusters, the total number of particles and the average number of particles in a cluster, respectively. In the case of the percolation problem, the moments are expressed using the critical exponents  $\alpha$ ,  $\beta$  and  $\gamma$  as follows:

$$M_0 \sim |p - p_c|^{2-\alpha} \quad M_1 \sim |p - p_c|^\beta \quad M_2 \sim |p - p_c|^{-\gamma}. \quad (5)$$

Therefore, the critical exponents satisfy the following universal relation:

$$\alpha + 2\beta + \gamma = 2. \quad (6)$$

Relation (6) is also obtained in thermo-magnetic and vapour-liquid second-order phase transition systems [12–14].

In the case of electron(s) in a two-quantum well system, the electronic wavefunction is localized in one quantum well (well 1) when the electric field is weak and it spreads over the two quantum wells (well 1 and 2) in the tunnelling electric field. The probability density in well 1 and 2, respectively, decreases and increases gradually as the electric field increases beyond the tunnelling electric field. The above electronic characteristics in a two-quantum well system is reminiscent of the classical percolation phenomenon as mentioned earlier. Therefore, in this paper, the SET phenomenon is analysed as if it were one type of percolation in a finite system and the scaling characteristics of the electronic probability densities for both one- and two-electron systems is investigated. We believe that it is worthwhile to examine if there are universal relations, which are independent of the system and quantum well sizes, in the SET phenomenon because it may be able to design a tunnelling device based on those universal relations. In section 2, the calculation model and method are described. In section 3, the results of the numerical calculation are shown and the scaling characteristics are discussed. A scaling analysis is also carried out and the result of the analysis compared with the numerical result. In the final section, the scaling law in electronic tunnelling is summarized.

## 2. Calculation model and method

The calculation model is shown in figure 1. The potential barrier (Region 3) is sandwiched between two quantum wells (Regions 1 and 2). The potential height of the edges of the quantum wells is infinite. The width of the barrier is 3 nm. The total length of the system is fixed at 63 nm and the combinations of the lengths of the two wells are changed as follows:  $(L_1, L_2 \text{ nm}) = (15, 45), (18, 42), (21, 39), (24, 36), (27, 33), (30, 30)$ . One or two electrons are placed in Region 1 initially. A dc electric field is applied to the system and the strength of the electric field is increased gradually. In the case of the one-electron system, the electron tunnels in a particular strength of electric field and the electronic probability in Region 2 increases with the electric field. In the case of the two-electron system, one electron tunnels in a critical electric field and the second electron also tunnels in a stronger electric field.

The steady-state Schrödinger equation corresponding to figure 1 is expressed as follows in atomic units:

$$H^\alpha \psi^\alpha(x_\alpha) = \epsilon^\alpha \psi^\alpha(x_\alpha) \quad (\alpha = 1, 2) \quad (7)$$

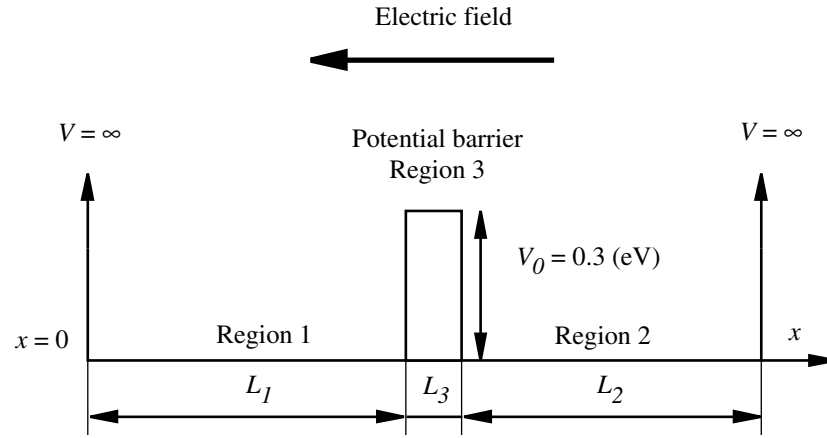


**Figure 1.** Calculation model. The potential barrier is sandwiched between two quantum wells. One or two electrons are placed in Region 1 initially. A dc electric field is applied and the strength is increased gradually.

where  $H$  is the Hamiltonian operator and  $\alpha$  represents electron 1 or 2:

$$H^\alpha \equiv -\frac{1}{2m} \frac{\partial^2}{\partial x_\alpha^2} + \int_{\beta \neq \alpha} dx_\beta \frac{|\psi^\beta(x_\beta)|^2}{|x_\beta - x_\alpha|} - \int_{\beta \neq \alpha} dx_\beta \frac{\bar{\psi}^\beta(x_\beta) P_{x_\alpha, x_\beta} \psi^\beta(x_\beta)}{|x_\beta - x_\alpha|} + V(x_\alpha) - E x_\alpha \quad (8)$$

where  $m$  is the effective mass of an electron and  $E$  is an external electric field. The second term on the right-hand side is the Coulomb energy and the third term is the exchange energy where  $P_{x_\alpha, x_\beta}$  is the exchange operator between  $x_\alpha$  and  $x_\beta$ .  $\bar{\psi}^\beta$  is the complex conjugate to  $\psi^\beta$ .  $V(x)$  is the potential of the system, which is summarized below:

$$V(x) = \begin{cases} \infty & \text{for } x = 0 \\ 0 & \text{for } 0 < x \leq L_1 & \text{(Region 1)} \\ V_0 & \text{for } L_1 < x < L_1 + L_3 & \text{(Region 3)} \\ 0 & \text{for } L_1 + L_3 \leq x < L_1 + L_2 + L_3 & \text{(Region 2)} \\ \infty & \text{for } x = L_1 + L_2 + L_3. \end{cases} \quad (9)$$

$m = 0.066$  au, which corresponds to an electron in GaAs, and  $V_0 = 0.3$  eV, which corresponds to the potential of  $\text{Al}_{0.3}\text{Ga}_{0.7}\text{As}$  in GaAs, are used in the following calculations. Equation (7) was solved by the QL method [15, 16] and the finite difference method where the spatial derivative was approximated by the central difference formula [17]. The calculation procedure is as follows: equation (7) is converted to an eigenvalue equation of a tridiagonal matrix by the finite difference formulation. The tridiagonal matrix is decomposed into a product of orthogonal and lower triangular matrices (QL algorithm) and the eigenvalues and eigenvectors are obtained efficiently by employing the shifting technique (see [15, 16] for details). In the case of the two-electron systems, the eigenvalues and eigenvectors are calculated under the potentials which were themselves derived from wavefunctions that had been obtained at the previous calculation step. This procedure is repeated until the following convergence criterion is satisfied:  $|\epsilon_{I+1}^\alpha - \epsilon_I^\alpha|/\epsilon_I^\alpha < 10^{-8}$ , where subscript I represents the iteration count. The calculation space was divided by 106, 211, 421 finite difference grid points. The differences

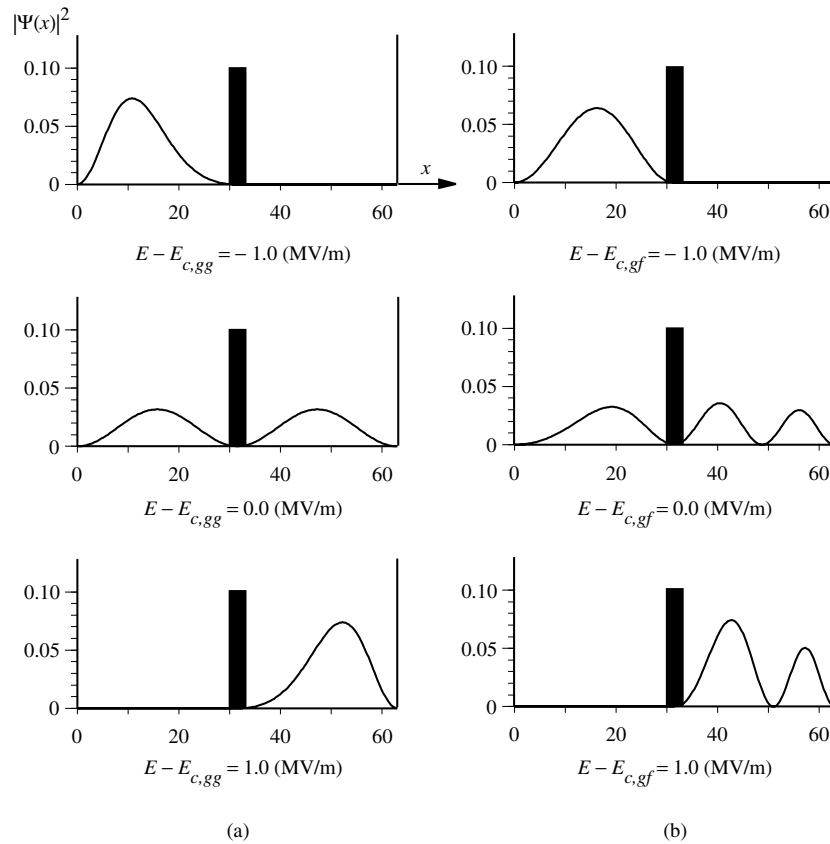


**Figure 2.** Electronic probability density in a one-electron system.  $L_1 = 30$ ,  $L_2 = 3$ ,  $L_3 = 30$  nm. (a) Ground-state to ground-state tunnelling.  $E_{c,gg} = 0$  V m $^{-1}$ ; (b) ground-state to first-excited-state tunnelling.  $E_{c,gf} = 0.57$  MV m $^{-1}$ .

in the values of the calculated wavefunctions caused by the grid number differences were within  $10^{-3}\%$ . The results shown in the following are based on the calculations with 211 finite difference grid points.

### 3. Results and discussion

In this section, we analyse electronic tunnelling phenomena in one- and two-electron systems and investigate the scaling characteristics.

#### 3.1. One-electron system

Two examples of the distributions of the electronic probability densities in the one-electron system are shown in figure 2 for  $L_1 = L_2 = 30$  nm. Figure 2(a) represents tunnelling from the ground-state in Region 1 to 2 and figure 2(b) from the ground-state in Region 1 to the first-excited-state in Region 2. One electron is placed in Region 1 initially (see figures 2(a) and (b),  $E - E_{c,gg} = -1.0$ ,  $E - E_{c,gf} = -1.0$  MV m $^{-1}$ ). When the strength of the electric field reaches a critical value, the electron tunnels through the barrier where the variance of the probability

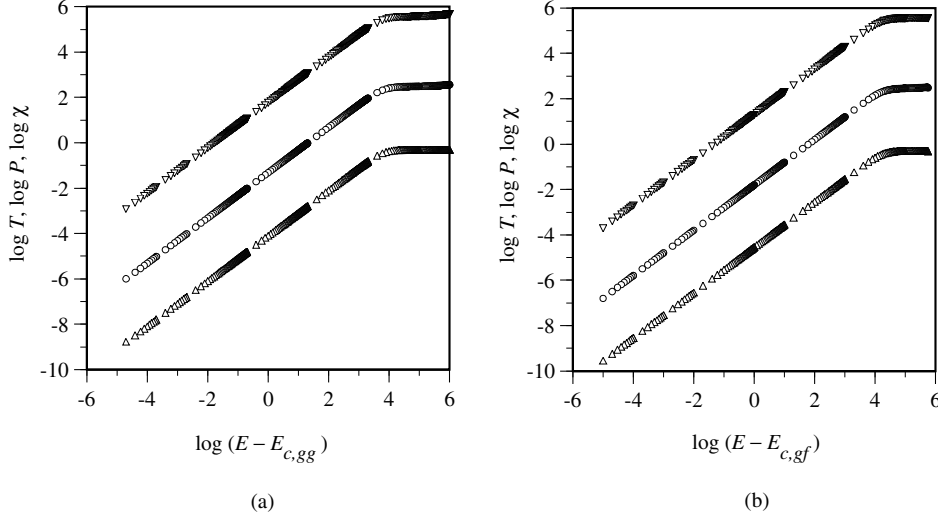


**Figure 3.** Dependence of the increase in the probability of electron in Region 2, the first moment and the second moment on the control parameter in a one-electron system. The unit of  $E - E_{c,gg}$  and  $E - E_{c,gf}$  is  $\text{V m}^{-1}$ . (a) Ground-state to ground-state tunnelling; (b) ground-state to first-excited-state tunnelling. ( $\Delta$ ) The increase in the probability of electron in Region 2,  $T$ . ( $\circ$ ) The increase in the first moment in Region 2,  $P$ . ( $\nabla$ ) The increase in the second moment in Region 2,  $\chi$ . Power laws apply to  $T$ ,  $P$  and  $\chi$  when the control parameter  $\xi$  is smaller than  $100 \text{ V m}^{-1}$ . The exponents  $\alpha$ ,  $\beta$  and  $\gamma$  defined by equation (14) satisfy the relation  $\alpha - 2\beta + \gamma = 0$ .

density of the electron becomes maximum ( $E - E_{c,gg} = 0.0$ ,  $E - E_{c,gf} = 0.0 \text{ MV m}^{-1}$ ) and the probability of electronic tunnelling to Region 2 increases as the electric field increases ( $E - E_{c,gg} = 1.0$ ,  $E - E_{c,gf} = 1.0 \text{ MV m}^{-1}$ ).

We defined the tunnelling electric field  $E_c$  as an electric field in which the variance of the probability density distribution of electron, that is, susceptibility, becomes maximum. We calculated the increase in the probability of electron appearing in Region 2,  $T$ , the first moment,  $P$ , and the second moment,  $\chi$ , which are defined as follows:

$$T \equiv \langle \psi | \psi \rangle_2 - \langle \psi_c | \psi_c \rangle_2 \quad (10)$$

$$P \equiv \langle \psi | x | \psi \rangle_2 - \langle \psi_c | x | \psi_c \rangle_2 \quad (11)$$

$$\chi \equiv \langle \psi | x^2 | \psi \rangle_2 - \langle \psi_c | x^2 | \psi_c \rangle_2 \quad (12)$$

where subscript 2 represents Region 2 and  $c$  corresponds to the tunnelling electric field. The difference between the strength of electric field  $E$  and that of the tunnelling electric field  $E_c$  was taken as the control parameter  $\xi$ :

$$\xi \equiv E - E_c. \quad (13)$$

The dependence of  $T$ ,  $P$  and  $\chi$  on  $\xi$  in the one-electron system is shown in figure 3 for  $L_1 = L_2 = 30 \text{ nm}$ . When  $\xi$  is smaller than  $100 \text{ V m}^{-1}$ , power laws apply to  $T$ ,  $P$  and  $\chi$ . The power laws are expressed using exponents  $\alpha$ ,  $\beta$  and  $\gamma$  as follows:

$$T \sim \xi^\alpha \quad P \sim \xi^\beta \quad \chi \sim \xi^\gamma. \quad (14)$$

We found that  $\alpha$ ,  $\beta$  and  $\gamma = 1$  in the cases of both the ground-state to ground-state tunnelling (figure 3(a)) and the ground-state to first-excited-state tunnelling (figure 3(b)) irrespective of the differences in the lengths of quantum wells.

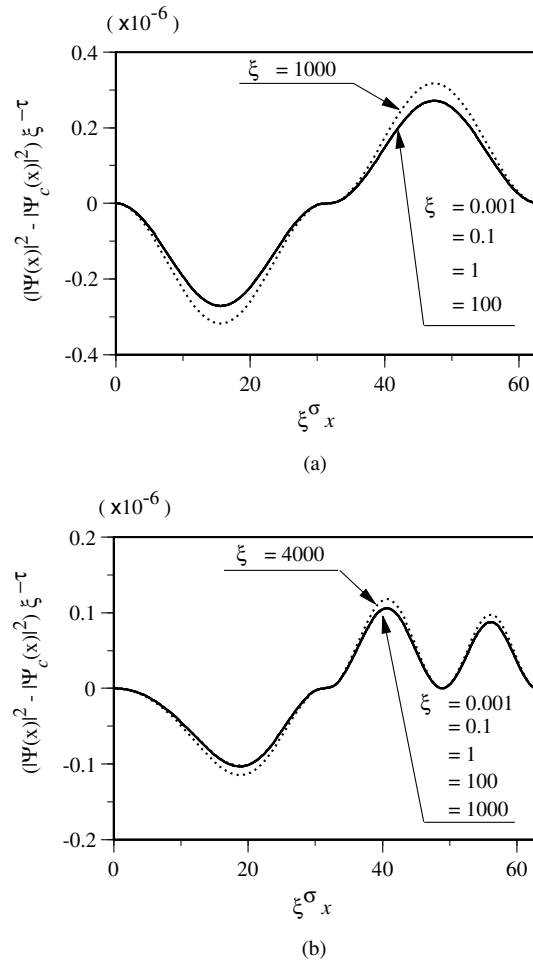


**Figure 4.** Scaling function  $f$  in a one-electron system. The unit of  $\xi$  is  $\text{V m}^{-1}$ . (a) Ground-state to ground-state tunnelling; (b) ground-state to first-excited-state tunnelling. The scaling function is defined by equation (15). When the control parameter is smaller than  $100 \text{ V m}^{-1}$ , the scaling function is universal for both the ground-state to ground-state and ground-state to first-excited-state tunnelling.

A scaling analysis was carried out in the following to explain the power law. It is assumed that the increase in the probability density of electron in Region 2,  $|\psi(x)|^2 - |\psi_c(x)|^2$ , is expressed by the following scaling relation:

$$|\psi(x)|^2 - |\psi_c(x)|^2 \sim \xi^\tau f(\xi^\sigma x) \quad (15)$$

where  $f$  is a scaling function. This relation corresponds to equation (1) in the case of the percolation scaling. The decrease in the probability density of electron in Region 1 is also scaled in the same manner as equation (15). Assuming equation (15) is correct, the following power relations are derived for  $T$ ,  $P$  and  $\chi$ :

$$T \sim \int_{\text{Region 2}} \xi^\tau f(\xi^\sigma x) dx = \xi^{\tau-\sigma} \int_{\text{Region 2}} f(z) dz \quad (\text{where } z \equiv \xi^\sigma x) \sim \xi^{\tau-\sigma} \quad (16)$$

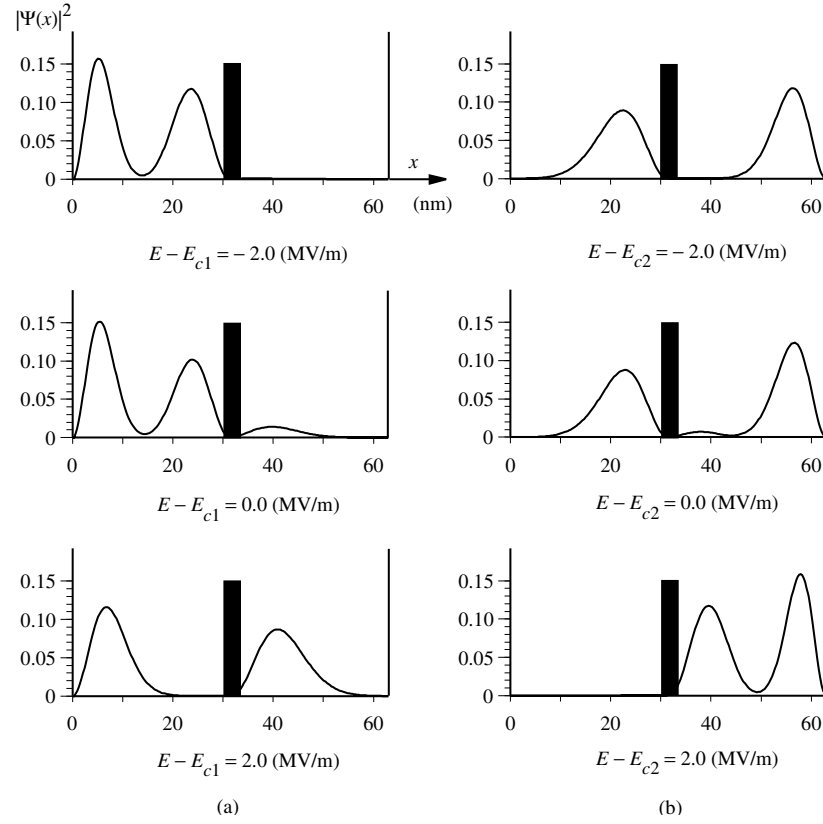


**Figure 5.** Electronic probability densities in a two-electron system.  $L_1 = 30$ ,  $L_2 = 3$ ,  $L_3 = 30$  nm. (a) First electron's tunnelling.  $E_{c1} = -3.11$  MV m $^{-1}$ ; (b) second electron's tunnelling.  $E_{c2} = 3.45$  MV m $^{-1}$ .

$$P \sim \int_{\text{Region 2}} x \xi^\tau f(\xi^\sigma x) dx \sim \xi^{\tau-2\sigma} \quad (17)$$

$$\chi \sim \int_{\text{Region 2}} x^2 \xi^\tau f(\xi^\sigma x) dx \sim \xi^{\tau-3\sigma}. \quad (18)$$

The above power relations (16)–(18) correspond to equations (2)–(4) in the case of the percolation scaling. Comparing equations (16)–(18) with (14), the following relations are obtained:

$$\alpha = \tau - \sigma \quad (19)$$

$$\beta = \tau - 2\sigma \quad (20)$$

$$\gamma = \tau - 3\sigma. \quad (21)$$

In general,  $\alpha$ ,  $\beta$  and  $\gamma$  satisfy the following relation:

$$\alpha - 2\beta + \gamma = 0. \quad (22)$$

If  $T$ ,  $P$  and  $\chi$  is expressed as in the case of the percolation scaling, that is,  $T \sim \xi^{2-\alpha}$ ,  $P \sim \xi^\beta$ ,  $\chi \sim \xi^{-\gamma}$  (see equation (5)), the relation (6);  $\alpha + 2\beta + \gamma = 2$ , is obtained. In the cases of both ground-state to ground-state and ground-state to first-excited-state tunnelling in the one-electron system,  $\tau = 1$  and  $\sigma = 0$ .



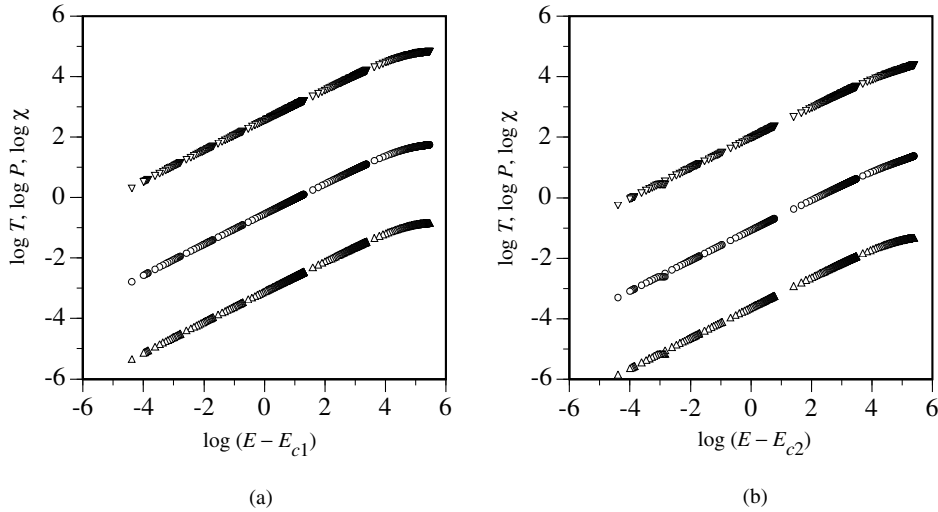


**Figure 6.** Dependence of the increase in the probability of tunnelling electron in Region 2, the first moment and the second moment on the control parameter in a two-electron system. The unit of  $E - E_{c1}$  and  $E - E_{c2}$  is  $\text{V m}^{-1}$ . (a) First electron's tunnelling; (b) second electron's tunnelling. ( $\Delta$ ) The increase in the probability of electron in Region 2,  $T$ . ( $\circ$ ) The increase in the first moment in Region 2,  $P$ . ( $\nabla$ ) The increase in the second moment in Region 2,  $\chi$ . Power laws also apply to  $T$ ,  $P$  and  $\chi$  when the control parameter  $\xi$  is smaller than  $100 \text{ V m}^{-1}$ . The exponents  $\alpha$ ,  $\beta$  and  $\gamma$  satisfy the relation  $\alpha - 2\beta + \gamma = 0$ .

The scaling function  $f$  is shown in figure 4 for  $L_1 = L_2 = 30 \text{ nm}$  as an example where the ordinate is  $(|\psi(x)|^2 - |\psi_c(x)|^2)\xi^{-\tau}$  and the abscissa is  $\xi^\sigma x$  (see equation (15)). When the control parameter is smaller than  $100 \text{ V m}^{-1}$ , the scaling function is universal irrespective of the values of the control parameter in both the ground-state to ground-state tunnelling and ground-state to first-excited-state tunnelling. The above scaling characteristics were also obtained for the different combinations of the lengths of quantum wells.

### 3.2. Two-electron system

Electronic probability densities in the two-electron system are shown in figure 5 for  $L_1 = L_2 = 30 \text{ nm}$ . Two electrons are placed in Region 1 initially (see figure 5(a),  $E - E_{c1} = -2.0 \text{ MV m}^{-1}$ ). One electron tunnels in a critical electric field where the variance of the probability density of the tunnelling electron becomes maximum (figure 5(a),  $E - E_{c1} = 0.0 \text{ MV m}^{-1}$ ). The probability density of the first electron tunnelling to Region 2 increases with the electric field (figure 5(a),  $E - E_{c1} = 2.0 \text{ MV m}^{-1}$ ). The other electron which stays in Region 1 tunnels to Region 2 in another critical electric field (figure 5(b),  $E - E_{c2} = 0.0 \text{ MV m}^{-1}$ ) and the probability density of the second electron found in Region 2 increases with the electric field (figure 5(b),  $E - E_{c2} = 2.0 \text{ MV m}^{-1}$ ).

The dependence of  $T$ ,  $P$  and  $\chi$  on  $\xi$  in the two-electron system is shown in figure 6 for  $L_1 = L_2 = 30 \text{ nm}$ , where figure 6(a) corresponds to the first electron's tunnelling and figure 6(b) the second electron's tunnelling. Power laws also apply to  $T$ ,  $P$  and  $\chi$  in the cases of both the first and second electrons' tunnelling when  $\xi$  is smaller than  $100 \text{ V m}^{-1}$ .  $\alpha$ ,  $\beta$  and  $\gamma = 0.5$  in both cases.

The scaling function defined by equation (15) is shown in figure 7. The scaling function  $f$  is universal when  $\xi$  is smaller than  $100 \text{ V m}^{-1}$  for both the first and second electrons'

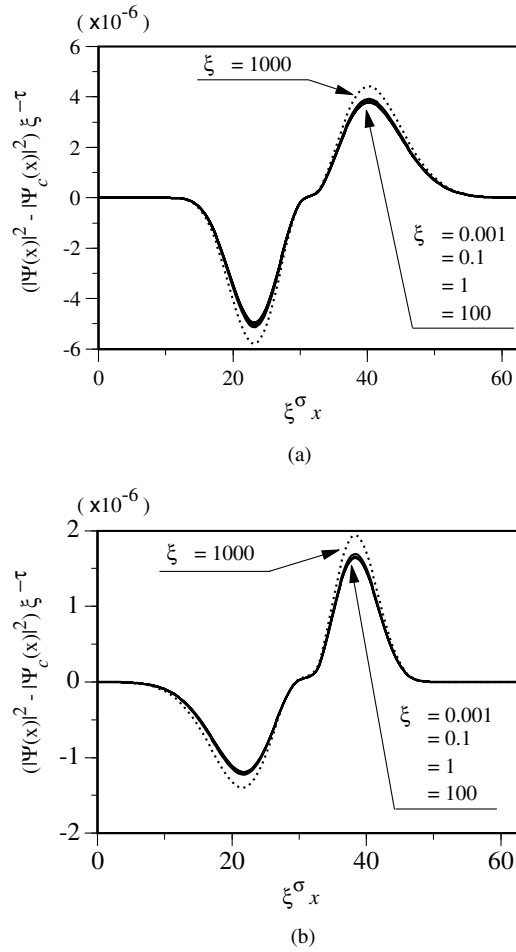


**Figure 7.** Scaling function  $f$  in a two-electron system. The unit of  $\xi$  is  $\text{V m}^{-1}$ . (a) First electron's tunnelling; (b) second electron's tunnelling. When the control parameter is smaller than  $100 \text{ V m}^{-1}$ , the scaling function is universal for both the first and second electrons' tunnelling.

tunnelling. Even in the two-electron systems where the strong nonlinear interaction between two electrons is taken into account, the scaling law still applies to the probability densities near the tunnelling electric field and, as a result, the power laws expressed by equation (14) are obtained.

### 3.3. Energy and entropy changes in the tunnelling electric field

We calculated the changes in the total energy and the information entropy as a function of the control parameter  $\xi \equiv E - E_c$ . The total energy of the system is calculated by equation (7). We also calculated the information entropy of the electronic probability densities,  $S$ , by the following equation:

$$S \equiv -\sum_i P_i \log P_i \quad (23)$$

where  $P_i$  is the probability of electron being found in finite difference Region  $i$ .

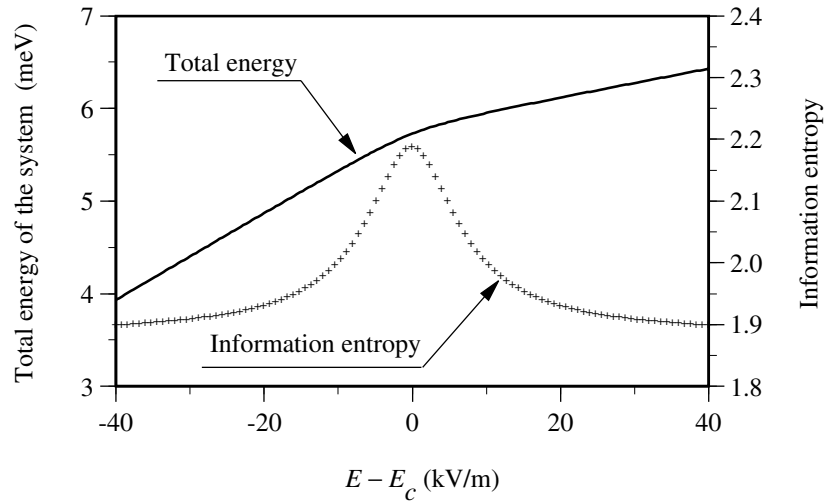


**Figure 8.** Dependence of total energy and information entropy on electric field in a one-electron system. The total energy and the information entropy change continuously in the tunnelling electric field.

The dependence of the total energy of the system and the information entropy of the electronic probability density on the external electric field is shown in figure 8 for a one-electron system of  $L_1 = L_2 = 30$  nm. The total energy and the entropy change continuously in the tunnelling electric field. The dependence of the total energy and the information entropy of the electrons' probability densities on the electric field is shown in figure 9 for a two-electron system of  $L_1 = L_2 = 30$  nm. The total energy and entropy change discontinuously for both the first and second electrons' tunnelling. Electronic tunnelling in one-dimensional systems is similar to a second-order transition, whereas electronic tunnelling in two-electron systems seems to be a first-order phase transition although electronic tunnelling phenomena are different from phase transitions.

Although the one- and two-electron systems are different in terms of the energy and entropy changes in the tunnelling electric field, a scaling relation expressed by equation (15) applies to both systems and therefore power laws apply to  $T$ ,  $P$  and  $\chi$  near the tunnelling electric field.

#### 4. Conclusion

We studied electronic tunnelling between two quantum wells in one- and two-electron systems numerically and the following results were obtained: (1) the increase of the probability density of tunnelling electron in a quantum well is scaled as  $|\psi(x)|^2 - |\psi_c(x)|^2 \sim \xi^\tau f(\xi^\sigma x)$  near the tunnelling electric field in both one- and two-electron systems, where  $f$  and  $\xi$  are, respectively, a scaling function and the difference between the electric field and the tunnelling electric field. (2) As a result, power laws apply to the increase of the tunnelling probability,  $T \equiv \langle \psi | \psi \rangle_2 - \langle \psi_c | \psi_c \rangle_2$ , the first moment,  $P \equiv \langle \psi | x | \psi \rangle_2 - \langle \psi_c | x | \psi_c \rangle_2$ , and the second moment,  $\chi \equiv \langle \psi | x^2 | \psi \rangle_2 - \langle \psi_c | x^2 | \psi_c \rangle_2$ , as  $T \sim \xi^\alpha$ ,  $P \sim \xi^\beta$ ,  $\chi \sim \xi^\gamma$  where the exponents satisfy  $\alpha - 2\beta + \gamma = 0$ . (3) The total energy of the system and the information entropy of the electronic probability density change continuously in the tunnelling electric field in the case of one-electron systems, whereas they change discontinuously in the tunnelling electric field in the case of two-electron systems.

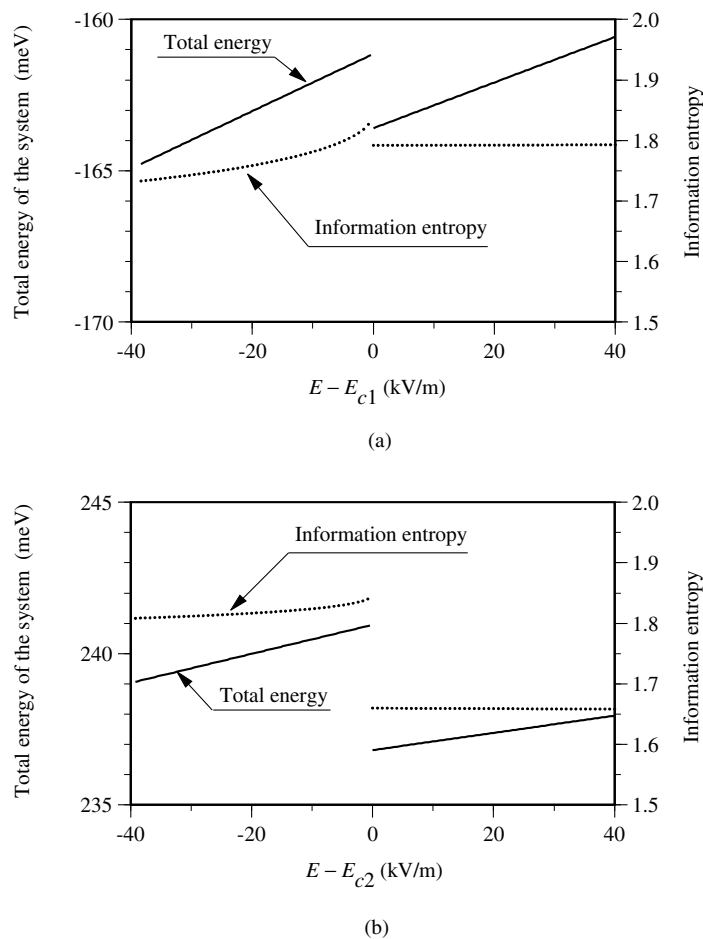


**Figure 9.** Dependence of total energy and information entropy on electric field in a two-electron system. (a) First electron's tunnelling; (b) second electron's tunnelling. The total energy and the information entropy change discontinuously in the tunnelling electric field in both the first and second electrons' tunnelling.

## Acknowledgments

This study has been supported by the High-Tech Research Centre organized by the Ministry of Education, Culture, Science and Sports, Japan, since 1997 and the Special Research Fund, Toyo University, since 1999. We would like to thank Professor Sugano, Toyo University, and Dr Hanajiri, Toyo University, for their constructive comments.

## References

- [1] Cappasso F and Datta S 1990 *Phys. Today* **43** 74
- [2] Kastner M A 1993 *Phys. Today* **46** 24
- [3] Ismail K, Antoniadis D A and Smith H I 1989 *Appl. Phys. Lett.* **55** 589
- [4] Tsukada N, Wieck A D and Ploog K 1990 *Appl. Phys. Lett.* **56** 2527
- [5] Wang J and Guo H 1993 *Phys. Rev. B* **48** 12 072

- [6] Field S B, Kastner M A, Meirav U, Scott-Thomas J H F, Antoniadis D A, Smith H I and Wind S J 1990 *Phys. Rev. B* **42** 3523
- [7] Meirav U, Kastner M A and Wind S J 1990 *Phys. Rev. Lett.* **65** 771
- [8] Beenakker C W J 1991 *Phys. Rev. B* **44** 1646
- [9] Grabert H and Devoret M H 1992 *Single Charge Tunneling Coulomb Blockade Phenomena in Nanostructures* (New York: Plenum)
- [10] Kastner M A 1992 *Rev. Mod. Phys.* **64** 849
- [11] Stauffer D and Aharony A 1998 *Introduction to Percolation Theory* (London: Taylor and Francis)
- [12] Stanley H E 1971 *Introduction to Phase Transitions and Critical Phenomena* (Oxford: Clarendon)
- [13] Gebhardt H 1980 *Phasenübergänge und Kritische Phänomene* (Braunschweig: Vieweg)
- [14] Ma S K 1996 *Modern Theory of Critical Phenomena* (Tokyo: Addison-Wesley)
- [15] Jennings A 1978 *Matrix Computation for Engineers and Scientists* (Chichester: Wiley)
- [16] Hill D R 1988 *Experiments in Computational Matrix Algebra* (New York: Random House)
- [17] Richardson J L 1991 *Comput. Phys. Commun.* **63** 84